



Semnan University



Energy and Exergy Analyses of a Diesel Engine Running on Biodiesel Fuel

Reza Bahoosh *, Mohammad Sedeh Ghahfarokhi, Mohammad Reza Saffarian

Department of Mechanical Engineering, Shahid Chamran University of Ahvaz, Ahvaz, Iran

PAPER INFO

Paper history:

Received: 2017-05-09

Received: 2017-10-13

Accepted: 2017-10-21

Keywords:

Exergy;
Availability;
Diesel Engine;
Nitrogen oxide;
Biodiesel.

ABSTRACT

Availability analysis is an effective approach to studying energy conversion in systems and identifying inefficiency. In the present study, a single-zone model was used to examine energy performance parameters and heat release rates. The governing equation of availability analysis was applied in the model, and the possibility of using biodiesel produced from sunflower oil as diesel engine was investigated via mathematical simulation. The different exergy components of pure diesel fuel and pure biodiesel were compared at different crank angles. Results indicated that combining the examined diesel engine with biodiesel fuel would decrease the energy and exergy efficiencies by about 2.72% and 2.61%, respectively. As a result, work exergy and heat transfer exergy decrease and exhaust gas exergy and irreversibility would increase. When biodiesel is replaced with diesel fuel, carbon monoxide decreases, carbon dioxide formation increases, and nitrogen oxide formation remains constant. However, considering the negligible decrease in the first- and second-law efficiencies of biodiesel fuel compared with the decrease in diesel fuel efficiencies, the former is regarded as a renewable fuel that produces less carbon monoxide. It can therefore serve as a substitute for diesel fuel.

DOI: 10.22075/jhmtr.2017.11293.1160

© 2018 Published by Semnan University Press. All rights reserved.

1. Introduction

One of the paramount requirements for satisfying global energy standards is the development of alternative energy sources. These types of resources are incorporated in plans to reduce the greenhouse gas emissions caused by fossil fuels. In this regard, alternatives to diesel engine fuel are becoming increasingly important since the use of such alternatives involves low consumption of petroleum reserves and facilitates the reduction of the environmental consequences of exhaust gases from petroleum-fueled engines. The use of alternative fuels, such as ethanol and pure (pure or gasoline additives) biogas and biodiesel (pure or diesel additives), as diesel fuel replacements has been considered in recent years [1, 2]. Substantial research has thus far been devoted to the effects of renewable

resources on the performance levels and emissions of biodiesel-fueled diesel engines. Xue et al. [3], reviewed studies on alternative fuels comprehensively. The authors found that the use of biodiesel considerably reduces hydrocarbon and carbon monoxide (CO) emissions at negligible power loss and increased fuel consumption. They also indicated that conventional diesel engines with minimal or no modifications could increase nitrogen oxide (NO_x) emissions. They concluded that using fuel blends with a small amount of biodiesel in place of petroleum diesel could help control air pollution without significantly sacrificing engine power and economy.

Engine performance and pollutant emission parameters are generally analyzed on the basis of the first law of thermodynamics, but this approach does not consider the quality of a

* Corresponding Author: R. Bahoosh, Department of Mechanical Engineering, Shahid Chamran University of Ahvaz, Ahvaz, Iran.
Email: bahoosh@scu.ac.ir

system's energy content. In a specific case, the first law of thermodynamics can be used to calculate the maximum potential of a system to produce useful mechanical work. For the accurate identification of system performance, however, such law must be used in conjunction with the second law of thermodynamics.

Van Gerpan and Shapiro [4] presented a second-law analysis of the combustion process in a diesel engine by using a single-zone model. The authors determined the effects of combustion timing, mass burning rate, and heat transfer rate on availability destruction. They also demonstrated chemical availability as a necessary requirement in accurately estimating irreversibility. Rakopoulos and Giakoumis [5] carried out a second-law analysis of a multi-cylinder turbocharged diesel engine in a single-zone thermodynamic model and calculated all exergy terms and fuel flow rate at every control volume of the cylinder. Sobiesiak et al. [6] conducted first- and second-law analyses of a spark ignition engine fueled by compressed natural gas (CNG). The results indicated that considerable exergy destruction in engine operation is associated with combustion and heat transfer and that the exergy destruction stemming from heat transfer is lower with CNG fueling [6]. Amjad et al. [7] performed an exergy analysis of homogeneous charge compression ignition with a blended fuel that consists of n-heptane and natural gas. The combustion was represented using a single-zone model. Jafarmadar [8] numerically analyzed the combustion of hydrogen with air at constant pressure conditions (1 bar), various air fuel ratios, and initial temperatures in a zero-dimensional single-zone model with a chemical kinetic mechanism. Zhang and Caton [9] simulated engine cycles, integrating the second law of thermodynamics into the simulation to evaluate the energy and exergy distribution of various processes in a low-temperature combustion diesel engine. The effects of exhaust gas recirculation level and injection timing on first and second law parameters were also considered. Andrés et al. [10] studied the potential for waste energy recovery from exhaust gases in a diesel passenger car mounted on a chassis dynamometer. Panigrahi et al. [11] experimentally investigated a four-stroke single-cylinder diesel engine fueled by a blend of Mahua oil methyl ester (MOME) and diesel. Sayin Kul et al. [12] carried out energy and exergy analyses of a single-cylinder water-cooled diesel engine that uses biodiesel, diesel, and bioethanol blends.

The present research aims to simulate the engine operation using a single-zone model.

Second law indicators, such as burned fuel exergy, indicated work exergy, exergy loss associated with heat transfer to walls, combustion irreversibility, thermomechanical exergy, chemical exergy, and total cylinder exergy, per cycle were evaluated in the simulation.

2. Governing equations and simulation method

2.1. First-law analysis

This article was implemented for an MT4-244 direct injection diesel engine, which specifications are shown in Table 1. Governing equations were solved for engine operations, from inlet valve closing (IVC) to exhaust valve opening (EVO), using FORTRAN code.

2.2. Single-zone combustion model

The Whitehouse model was used to calculate the mass burning rate [13]. In this work, the preparation rate is given by:

$$P_n = \dot{K} (M_i)_n^{\frac{1}{3}} M_u^{\frac{2}{3}} P_{O_2}^X \quad (1)$$

Where M_i is the total mass (kg) of injected fuel up to time t (corresponding angle φ), \dot{K} and X are constants, P_{O_2} denotes the partial pressure of oxygen (O_2) (bar), and M_u represents the total mass (kg) of unprepared fuel. The term M_u can be written in the following form:

$$M_u = (M_i)_n - (P_{tot})_{n-1} \quad (2)$$

This alternative expression of M_u was established by introducing a chemical reaction rate on the basis of an Arrhenius-type expression. Under the assumption that the velocity of gas molecules is proportional to the square root of temperature, the density of O_2 is proportional to partial pressure divided by temperature. This phenomenon can be expressed as follows [13]:

$$R_n = k \frac{P_{O_2}}{N_{rpm} \sqrt{T}} \text{Exp} \left(\frac{-E_{act}}{T} \right) \int [(P_r)_n - (R)_{n-1}] d\varphi \quad (3)$$

Where R is the reaction rate (kg per degree), N is the engine speed in rev/min. Constant k and E_{act} are obtained from an analysis of indicator diagrams. During the early stages of the combustion process, the fuel burned at a time step dt ($^\circ\text{CA}$ step $d\varphi$) is controlled by the reaction rate.

$$dm_f = R_n \Delta\varphi \quad (4)$$

By contrast, after the progression of a short period of time, the fuel burned is controlled by preparation rate P .

$$dm_f = P_n \Delta\varphi \quad (5)$$

Table 1: Engine specifications [23]

Parameters	Specifications
Bore (mm)	100
Stroke (mm)	127
Displacement (cc)	3990
Compression ratio	17.5
Length of connecting rod (mm)	219
IVC (CA)	-145
EVO (CA)	+150
Engine speed (rpm)	1400

2.3. Heat transfer model

Simple correlations have been extended to internal combustion engines, with some of the most widely known equations being those developed by Woschni [14].

$$\frac{dQ_w}{dt} = hA(T_g - T_w) \quad (6)$$

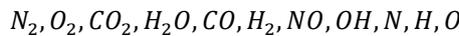
$$h = 3.26B^{-0.2}P^{-0.8}T^{-0.53}W^{0.8},$$

$$W = C_1S_P + C_2 \frac{V_d T_r}{P_r V_r} (P - P_m) \quad (7)$$

Velocity W is not an actual fluid speed but it is an equivalent value which would be obtained by matching calculated values with measurements under the main assumption that fluid flow in a cylinder is proportional to mean piston speed.

2.4. Chemistry of combustion

Combustion products are defined on the basis of dissociation considerations. For a C-H-O-N system, the complete chemical equilibrium scheme proposed by Olikara et al. [15] was utilized. The following 11 species were included in the calculations:



For the burning zone, the concentration of all above-mentioned species can be calculated by solving a system of equations consist of nonlinear four atom balance equations (one for each element) and seven equilibrium equations [15]. This calculation is prompted by the volume, temperature, mass of burned fuel, and mass of air entrained in the burning zone. The established equations were solved in this subsection through the Newton-Raphson iteration method.

2.5. Internal energy

In order to evaluate the specific internal energy of species (j) in Eq. (8), the polynomial function of (T) can be applied following Benson [14]; thus:

$$\frac{h_j(T)}{R_{mol}T} = \lambda_{j,0} + \lambda_{j,1}T + \lambda_{j,2}T^2 + \lambda_{j,3}T^3 + \lambda_{j,4}T^4 \quad (8)$$

$$u_j(T) = h_j(T) - R_{mol}T \quad (9)$$

2.6. Second-law analysis

For second-law analysis, the key concept is exergy. The exergy of a system is defined as the maximum value of work when a system reaches thermal, mechanical, and chemical equilibrium with its environment. This state of equilibrium is defined as the dead state of the system and depends on the pressure, temperature, and composition of the surrounding environment. The total exergy of a system is determined as follows [4, 16]:

$$A = A_{ch} + A_{th} = (E - U_0) + P_0(V - V_0) - T_0(S - S_0) = E + P_0V - T_0S - \sum_{j=1}^n n_j \mu_{0,j} \quad (10)$$

In the above expression, the kinetic and the potential energy are disregarded, and subscript 0 is related to the dead state.

2.7. Thermomechanical exergy

Thermomechanical exergy pertains to the available work of a substance in a system, as derived from the system initial temperature and pressure to the final temperature and pressure related to the dead state [4, 17].

$$A_{tm} = (U - U^0) + P_0(V - V^0) - T_0(S - S^0) = U + P_0V - T_0S - \sum_{j=1}^n n_j \mu_j^0 \quad (11)$$

3. Chemical exergy

Chemical exergy is characterized as the maximum work to be obtained when a system of interest reacts with reference substances present in the environment [4, 18].

$$A_{ch} = A - A_{tm} = \sum_{j=1}^n n_j (\mu_j^0 - \mu_{0,j}) \quad (12)$$

where μ_j^0 is the chemical potential of species j at the true dead state.

3.1. General Exergy balance equation

On the basis of crank angle, the exergy balance equation applied in closed systems inside the cylinder of a direct injection engine is expressed as follows [4, 16, 19]:

$$\frac{dA}{d\varphi} = -\frac{dA_w}{d\varphi} - \frac{dA_Q}{d\varphi} - \frac{dI}{d\varphi} + \frac{dA_f}{d\varphi} \quad (13)$$

Maximum work is defined as the availability of a system to do actual work on a changing control volume against its surroundings. In the above equation, A_w is the availability associated with the work done by a system which could be defined as the following equation:

$$\frac{dA_w}{d\phi} = (P - P_0) \frac{dV}{d\phi} \quad (14)$$

where P , is the instantaneous cylinder pressure, $dV / d\phi$ is the rate of change in cylinder volume with crank angle, and A_Q is the availability associated with heat transfer across a system boundary. The Woschni [14] correlation is extensively used in determining the convective heat transfer coefficient within an internal combustion engine. It is a function of cylinder pressure, gas speed, and cylinder bore. Its variation with crank angle is depicted by:

$$\frac{dA_Q}{d\phi} = \left(1 - \frac{T}{T_0}\right) \frac{dQ}{d\phi} \quad (15)$$

where A_Q is the work developed by a reversible power cycle that receives Q at temperature T and discharges energy via heat transfer to the environment at T_0 . A_f is the exergy associated with fuel combustion in a cylinder. Its variation with crank angle is expressed as:

$$\frac{dA_f}{d\phi} = \frac{dm_f}{d\phi} a_f \quad (16)$$

where A_f is the fuel exergy, and m_f denotes the mass of burned fuel.

The specific chemical exergy per unit mass of liquid fuels $C_\alpha H_\beta O_\gamma$ can be evaluated using the following expression [20]:

$$a_f = LHV_f \left[1.0401 + 0.1728 \frac{\beta}{\alpha} + 0.0432 \frac{\gamma}{\alpha} \right] \quad (17)$$

in which I is the destruction exergy associated with the combustion process in a cylinder. Its variation with crank angle is reflected as follows:

$$\frac{dI}{d\phi} = -\frac{T_0}{T} \sum_{j=1}^n \mu_j \frac{dn_j}{d\phi} \quad (18)$$

where index j stands for all reactants and products. For perfect gases, $\mu_j = g_j$ and $n_j = m_j$, and for fuel, $\mu_f = a_f$. The above equation indicates that both the heat transfer and work production in a cylinder affect only the irreversibility value.

3.2. Energy and exergy efficiencies

Efficiency is characterized to compare different engine size applications or evaluate numerous improvement effects based on either the first or the second law [20, 21]:

Table 2: Fuel properties [23]

Fuel properties	Diesel	Biodiesel
Molecular formula	$C_{16}H_{30}$	$C_{20}H_{39}O_2$
Lower heating value ($\frac{mj}{kg}$)	42.57	41.97
Cetane number	57.33	62.1
VES ($mm^2 \cdot s^{-1}$)	2.45	6.482
Mass mole (gr)	226	311
Oxygen content	0	10.5
Carbon content	85	77
Hydrogen content	15	12.5

$$\eta_I = \frac{W_{net}}{m_f LHV} \quad (19)$$

Second-law efficiency can be defined as the ratio of indicated work to the total chemical availability of fuel [19].

$$\eta_{II} = \frac{A_w}{m_f A_f} \quad (20)$$

3.3. Biodiesel (ethyl ester sunflower oil) analysis

As previously stated, this study used a single-zone model of a diesel engine supplied with biodiesel fuel to predict engine performance on the basis of the first and second laws of thermodynamics and exhaust emissions from the engine.

The polynomial equation coefficients [15] employed to determine specific heat (at constant pressure) and internal energy versus temperature data were obtained using the specialized software programs Gaussian 98 and Gaussian 03; Ref. [25] was also used as the basis in the derivation. In order to acquire data for training and testing the proposed model, a four-stroke diesel engine was supplied with a combination of biodiesel fuel (ethyl ester sunflower oil) and diesel fuel. The properties of the biodiesel produced from ethyl ester sunflower oil were measured using ASTM standards (Table 2).

4. Results and discussion

4.1. First-law results

The simulated pressure values were compared with those derived from experimental tests on the diesel and biodiesel supplied to the examined compression-ignition (CI) engine.

The comparison of the calculated pressures with the corresponding experimental data on the biodiesel fuel is illustrated in Figure 1a, which indicates good

agreement between the predicted values and data obtained from the experimental works [6, 23]. The discrepancy in peak pressure between the experiment and computation for the biodiesel is less than 1%. Note that the engine was injected with fuel near the top dead center (TDC) (1° before the TDC, late injection of fuel plus). The pressure curve near the TDC (first peak) decreases in comparison with the experimental output, and a small amount of fuel premixed with flame and fuel can release a certain amount of energy. A tangible effect on the second peak pressure curve was also observed. When the piston moves from the TDC to the bottom dead center (BDC), pressure should decrease because of gas expansion. However, the results indicated that energy release rate increases, thereby elevating pressure. The performance of the examined engine was designed on the basis of single-stage injection before and after the TDC. Fuel injection after the TDC reduces NO_x and indicator power. Fuel injection before the TDC would optimize the performance and could reduce soot formation [6, 23].

Figure 1b illustrates the replacement of diesel fuel with biodiesel. The use of the former in the cylinder, causes peak pressure to vary from 82.5 to 85 bar. An increase in viscosity, an increase in cetane number, and a reduction in ignition delay hasten combustion and thereby would strengthen maximum pressure.

Figure 2a illustrates the cylinder temperatures at different crank angles. The maximum temperature of the biodiesel fuel is greater than that of the diesel fuel. By reaching the biodiesel fuel to its maximum temperature, it expands at a lower temperature than that required to expand the diesel fuel because of the decreased gas pressure in the former. This phenomenon is attributed primarily to the decrease in temperature, the percentage of O_2 in the molecular structure of the biodiesel, and the earlier combustion and longer expansion of the biodiesel.

As shown in Figure 2b, the emission of CO is caused by incomplete combustion under lack of O_2 in the combustion of organic materials. CO emission is highest during the combustion process, but CO is converted into carbon dioxide (CO_2) upon fuel expansion and at a lower temperature of the process. Figure 2c illustrates what drives increased CO_2 . This increase results in more O_2 and lower amounts of CO emission from the biodiesel than from the diesel fuel. These results indicate that biodiesel fuel is a renewable source of energy.

High temperatures, especially in regions containing O_2 , and the time spent of combustion are very conducive to NO_x formation. The amounts of N_2 and O_2 in the aforementioned regions are equally effective factors for NO_x formation [24]. Figure 2d indicates that NO_x variations depend on the crank

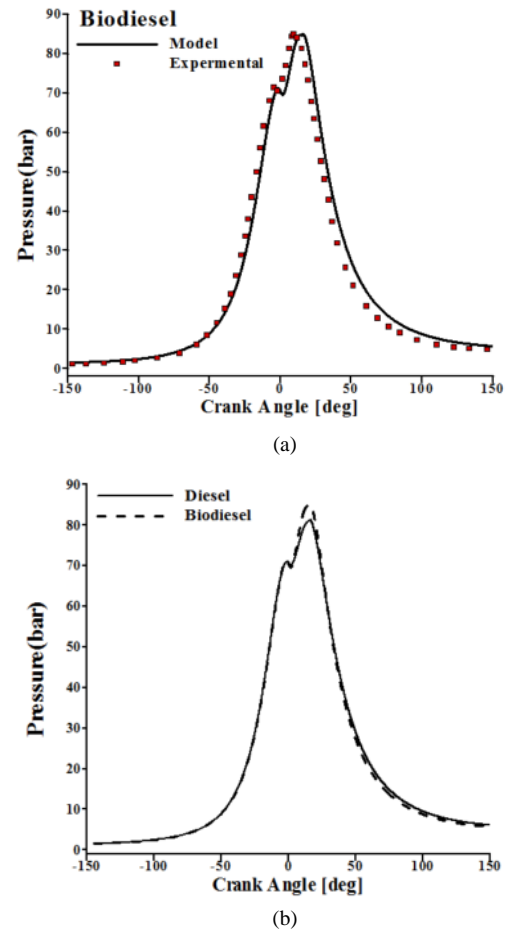


Figure 1. Comparison of (a) experimental pressure [6, 23] and simulated pressure for biodiesel fuel; (b) simulated pressure for diesel and biodiesel.

angle of the examined engine. An increase in temperature after combustion elevates NO_x emissions from the biodiesel fuel. All the factors that facilitate and accelerate the reaction between O_2 and N_2 increase NO_x formation. These factors include engine speed, the contents of a combustion chamber, the homogeneity of a combustion chamber, and mixture density in a combustion chamber. Nevertheless, the main factor for NO_x formation is the temperature. With decreasing temperature during the expansion of biodiesel fuel, negligible emission reduction would be achieved.

4.2. Second-law results

Figures 3a and 3b show the variations in both rate of exergy and cumulative exergy components versus crank angle for the biodiesel fuel at 1400 rpm (engine speed). The variation in chemical exergy during compression is constant. At this stage, minimal chemical exergy exists as a result of the presence of environmental species in the mixture. This process continues until the initiation of fuel injection into the combustion chamber. During fuel injection into the chamber, the chemical exergy variation in the system increases. Subsequently, the

conversion of the unburned species into combustion products rapidly would decrease the chemical exergy. At the end of the expansion, the amount of oxidizable and reducible chemical exergy from the unburned species is negligible.

Figure 4a shows the maximum work potential during the engine cycle. Maximum work is defined as the integration of respective terms over the entire crank angle of the engine in a cycle. Rapid combustion generates high cylinder pressure gradients, thereby enabling high maximum work. The maximum work levels over an entire cycle for the diesel fuel and biodiesel are 880.70J and 835.75J, respectively.

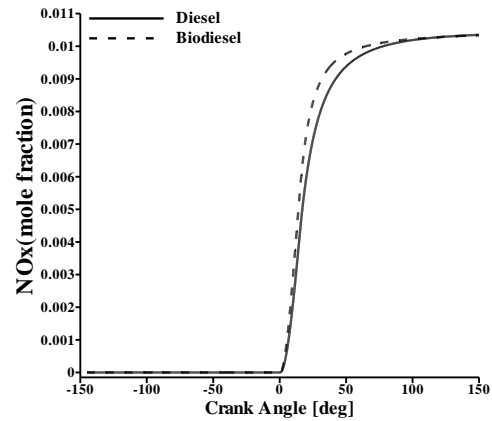
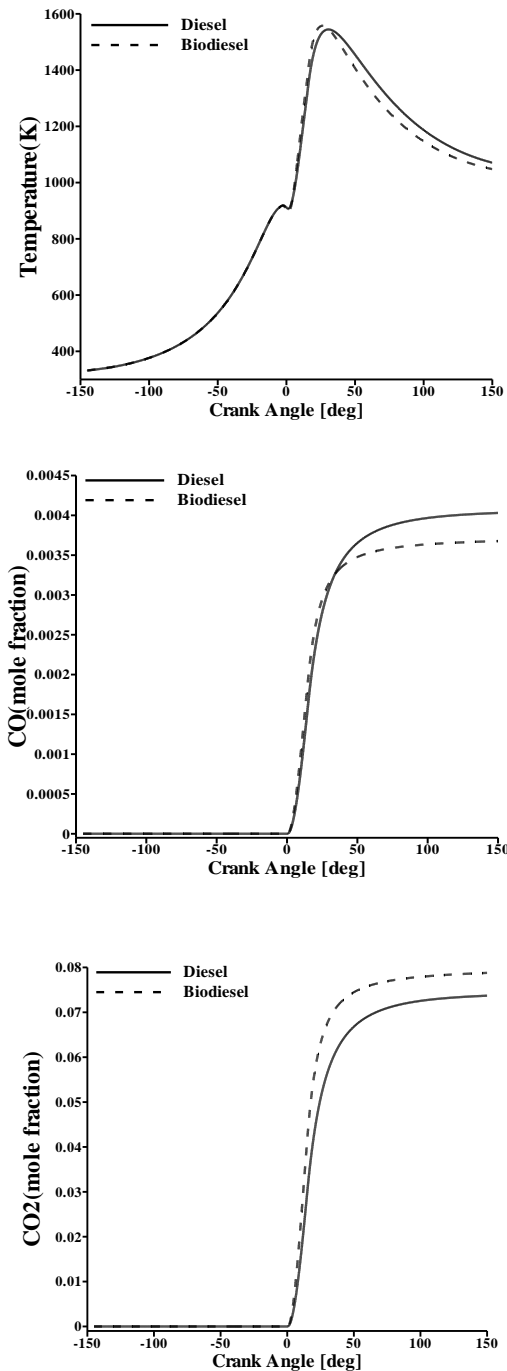


Figure 2. Comparison of diesel and biodiesel fuel predictions of (a) temperature (b) CO, (c) CO₂, and (d) NO_x at various crank angle positions.

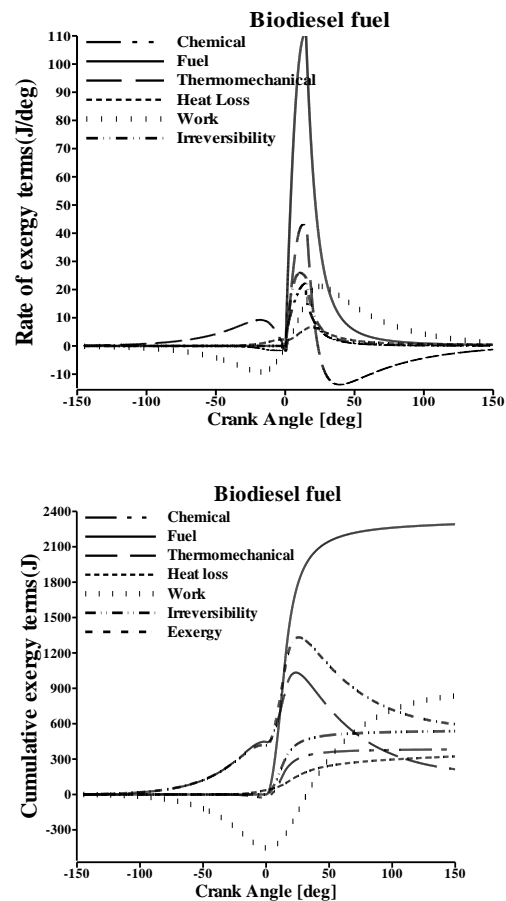


Figure 3. (a) Variations in exergy components of biodiesel fuel; (b) variations in cumulative exergy components of biodiesel fuel.

Volume reduction and gas pressure increase in the cylinder during the compression stroke can increase the work exergy. With the initiation of fuel injection, gas pressure begins to decrease. With the

initiation of combustion, pressure increases, and beyond the TDC, work exergy rapidly would increase. After fuel combustion is completed, work exergy increases until the end of the expansion stage given the reduction in pressure and the tendency of expansion stage to push the system towards the environment.

Figure 4b illustrates the development of cumulative heat loss exergy in the cylinder during the engine's closed cycle. Immediately after the start of combustion, the increase in the heat loss exergy of the biodiesel fuel is higher than that of the diesel fuel. This finding is ascribed to the higher pressure and temperature in the combustion stroke. The combustion stage exerts the greatest effect on the destruction of exergy because of the heat transfer in both fuels.

During the expansion stroke, the rate of change in the heat loss exergy of the biodiesel is smaller than that of the diesel fuel, but such rate is greater for the biodiesel in the combustion process. The accumulative heat loss exergy levels of the diesel fuel and biodiesel fuel are 329.64 and 322.72 J, respectively.

Figure 5a indicates the development of cumulative fuel exergy during a closed cycle. With the commencement of combustion based on the Whitehouse model and Eq. (4) or Eq. (5), the amount of fuel that is ready in the ignition delay stage is ignited immediately. At the beginning of combustion, therefore, fuel exergy rapidly increases. With the O₂ reduction caused by the increase in burned fuel, the fuel exergy rate declines. Biodiesel has a lower fuel heating value, lower viscosity, and higher density than diesel. In other words, the plungers for injection would pump more fuel into the cylinder. In ignition stage delay, then, more combustible fuel is at the ready, thereby leading to higher biodiesel fuel exergy than diesel fuel exergy. This result is consistent with the conclusions drawn by majority of the researchers. The accumulative burned fuel exergy levels of the diesel fuel and biodiesel fuel are 2273.65J and 2290.99J, respectively.

As shown in Figure 5b, the piston moves toward the TDC, and the volume of gas in the cylinder decreases. Pressure and gas temperature also begin to increase, which results in elevating the thermomechanical exergy. As ignition delays, temperature and pressure decreases, and when combustion begins, temperature and pressure rise, thereby it would cause augmenting the thermomechanical exergy. The system tends to reach environmental temperature and pressure, consequently reducing thermomechanical exergy.

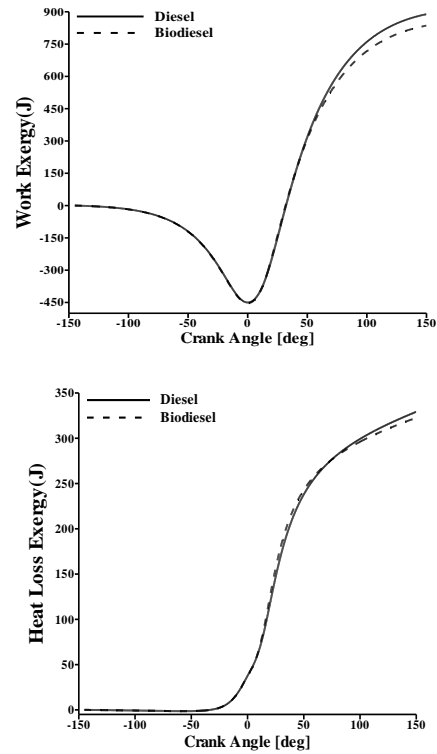


Figure 4. Variations in cumulative (a) work exergy and (b) heat loss exergy of biodiesel and diesel with crank angle position.

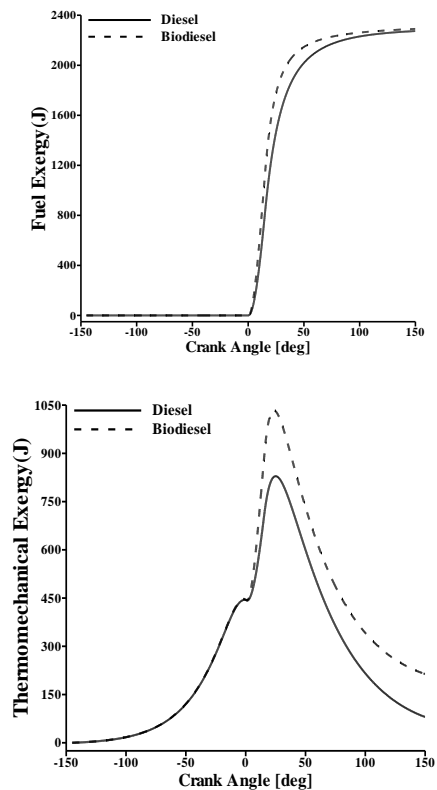


Figure 5. Variations in cumulative (a) fuel cylinder exergy and (b) thermomechanical cylinder exergy of biodiesel and diesel with crank angle position.

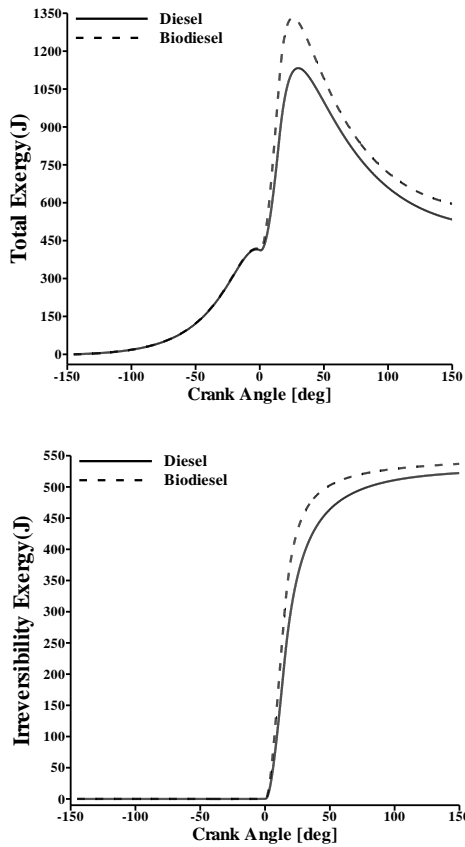


Figure 6. Variations in cumulative (a) total cylinder exergy and (b) irreversibility cylinder exergy of biodiesel and diesel fuel with crank angle position.

The thermodynamic conditions of the system and the environment are closer, and thermomechanical exergy is close to zero (Figure 3a). The thermomechanical exergy of the biodiesel fuel is greater than that of the diesel fuel because of the maximum temperature and pressure of the former in comparison with that of the latter. At the end of the expansion stroke, the accumulative thermomechanical exergy levels of the diesel fuel and biodiesel fuel are 80.20J and 213.68J, respectively.

The analysis of different components of Eq. (13), the prevalence of fuel chemical exergy over the change in work exergy, heat transfer, and irreversibility in the process of combustion and combustion trail indicates that total exergy would change. Total exergy is a component of the fuel exergy that is accessible and useful; this part of the exergy system exits through the exhaust gases emitted by a cylinder used in a turbocharged system.

Figure 4a and the evaluated components of exergy indicate that biodiesel fuel has less fuel exergy to be converted into work and heat transfer exergy than diesel fuel. Thus, the total exergy of the biodiesel fuel throughout the cycle is greater than that of the diesel fuel. Figure 6b demonstrates the destroyed

availability (irreversibility) as a function of crank angle for the diesel and biodiesel fuels. Irreversibility starts from zero and then increases to its final value during the combustion process. Eq. (18) illustrates that the accumulated irreversibility in each fuel depends on the mass of the fuel that is burned during combustion. Thus, the accumulated irreversibility of the biodiesel fuel is higher than that of the diesel fuel.

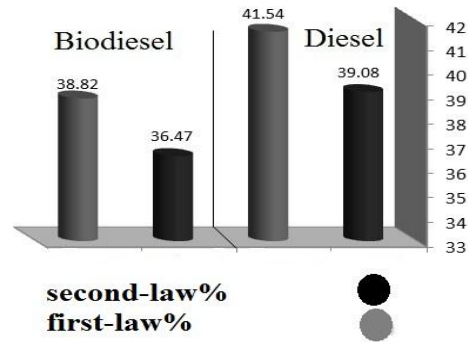


Figure 7. First- and second-law efficiencies of diesel and biodiesel.

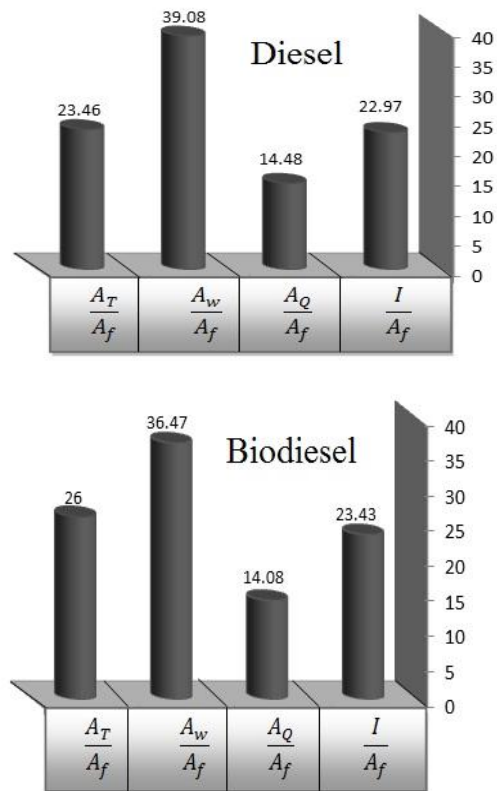


Figure 8. Comparative exergy distributions of (a) diesel and (b) biodiesel.

4.3. First and second-law efficiencies

Figure 7 shows the first- and second-law efficiencies of the diesel and biodiesel fuels. When the biodiesel is used as an alternative to the diesel fuel, the first-law efficiency decreases by 2.72% (i.e., from 41.54% to 38.82%), and the second-law

efficiency declines by 2.61% (i.e., from 39.08% to 36.47%). Using the biodiesel fuel would decrease the absolute value of indicated work or availability; however, fuel exergy increases (Figure 5a). Figure 8 depicts the exergy term-to-fuel exergy ratio of the biodiesel and diesel fuels.

5. Conclusion

A single-zone combustion model was developed in this study for first- and second-law analyses of a CI engine supplied with diesel and biodiesel fuels. Various availability components were calculated separately as a function of crank angle. CO₂ increases, whereas CO decreases when biodiesel is used as the engine fuel. The results of the exergy analysis of the diesel- and biodiesel-fueled engines are summarized as follows. A total of 39.08% of the intake fuel exergy of the diesel fuel is converted into useful work, whereas 36.47% of the intake fuel exergy of the biodiesel fuel is converted into the useful work. In the biodiesel-fueled engine, 14.08%, 23.43%, and 26% of the intake fuel exergy are converted into heat loss exergy, irreversibility, and exergy as byproducts of combustion, respectively. In the diesel-fueled engine, 14.48%, 22.97%, 23.64% of the fuel exergy is changed into heat loss exergy, irreversibility, and exergy as byproducts of combustion.

Finally, the analysis showed that the viscosity and density of biodiesel is a limiting factor for appropriate combustion in a CI engine. In practice, this would lead to the incomplete atomization of spraying fuel. The mixing of pure biodiesel fuel with air would create a non-homogeneous equivalence ratio in the combustion chamber, thereby causing incomplete combustion and low efficiency. Thus, because of the negligible decrease in the first- and second-law efficiencies of biodiesel fuel, it can serve as a substitute for diesel fuel under the same performance conditions.

Nomenclature

A	Availability
BDC	Bottom dead center
C	Heat transfer coefficient of Woschni
CA	Crank angle
CI	Compression-ignition
CO	Carbon monoxide (pollution)
E	Total energy
Eact	Reduced activation energy
EVO	Exhaust valve opening
G	Gibbs function
h	Convective heat transfer Coefficient
I	Irreversibility
IVC	Inlet valve closing
K	Preparation constant in the Whitehouse model
K	Reaction rate constant in the Whitehouse model
LHV	Fuel lower heating value

N	Engine speed
Q	Heat transfer
S	Entropy
TDC	Top dead center
u	Internal energy
W	Work

Greek symbols

φ	Crank angle
-----------	-------------

Subscripts

ch	Chemical
f	Fuel
r	Reference conditions
w	Wall

References

- [1] DK Birur, TW Hertel and WE Tyner, The Biofuel Boom: Implications for World Food Markets. Paper presented at the Food Economy Conference, The Hague. (2007).
- [2] S. Ramadhas, S. Jayaraj and C. Muraleedharan, Theoretical Modeling Experimental Studies on Biodiesel-Fueled Engine, *Renewable Energy*, 31, 1813-1826 (2006).
- [3] J. Xue, T. E. Grift and A. CHansen, Effect of Biodiesel on Engine Performances and Emissions, *Renewable and Sustainable Energy Reviews*, 15, 1098-1116 (2011).
- [4] J. H. Van Gerpen, and H. N. Shapiro, Second-law Analysis of Diesel Engine Combustion, *Trans ASME J Eng. Gas Turbines Power*, 112, 129-137, (1990).
- [5] C. D. Rakopoulos and E. G. Giakoumis, Development of Cumulative and Availability Rate Balances in A Multi-Cylinder Turbocharged IDI diesel Engine, *Energy Convers Manage*, 38, 347-369, (1997).
- [6] Sobiesiak and S. G. Zhan, The First and Second Law Analysis of Spark Ignition Engine Fuelled with Compressed Natural gas, *SAE Technical paper*, 2003-01-3091, (2003).
- [7] K. Amjad, Availability Analysis of N-Heptane and Natural Gas Blends Combustion in HCCI Engines, *Energy*, 36, 6900-6909, (2011).
- [8] S. Jafarmadar, The Numerical Exergy Analysis of H₂/air Combustion with Detailed Chemical Kinetic Simulation Model, *Int. J. Engineering*, 3(25), 239-48, (2012).
- [9] J. Zheng and J. A. Caton, Second Law Analysis of a Low Temperature Combustion Diesel Engine: Effect of Injection Timing and Exhaust Gas Recirculation, *Energy*, 38, 78-84, (2012).

- [10] Andrés and G-C. Reyes, A. John, A. Octavio, Potential for Exhaust Gas Energy Recovery in a Diesel Passenger Car Under European Driving Cycle, *Applied Energy*, 174, 201–212, (2016).
- [11] N. Panigrahi, M. K. Mohanty, S. R. Mishra, and R. C. Mohanty, Energy and Exergy Analysis of a Diesel Engine Fuelled with Diesel and Simarouba Biodiesel Blends, *Institution of Engineers*, 1-9, (2016).
- [12] Sayin Kul and A. Kahraman, Energy and Exergy Analyses of a Diesel Engine Fuelled with Biodiesel-Diesel Blends Containing 5% Bioethanol, *Entropy*, 174, 201–212, (2016).
- [13] S. Benson Rowland and N. D. Whitehouse *Internal Combustion Engines, Volume 2.*
- [14] *Thermodynamics and fluid mechanics series* Publisher Pergamon Press, (1979).
- [15] G. Woschni, Universally Applicable Equation for Instantaneous Heat transfer Coefficient in The Internal Combustion Engine, SAE Technical Paper, No. 670931, Published 01 Feb, (1967).
- [16] Olikara, G. L. Borman, A Computer Program for Calculating Properties of Equilibrium Combustion Products with Some Application to I.C Engine, SAE Technical Paper, No. 750468. (1975).
- [17] M. J. Moran and H. N. Shapiro, *Fundamentals Engineering Thermodynamics*, 5th Edition, England, John Wiley, (2006).
- [18] D. Rakopoulos, G. Giakoumis, *Diesel Engine Transient Operation*, 1st Edition, illustrated, Springer (2009).
- [19] C. D. Rakopoulos, C. N. Michos and E. G. Giakoumis, Availability Analysis of A Syngas Fueled Spark Ignition Engine Using a Multi-Zone Combustion Model, *Energy*, 32, 1378-1398 (2008).
- [20] C. D. Rakopoulos and E. G. Giakoumis, Second-Law Analyses Applied to Internal Combustion Engines Operation, *Prog. Energy Combust Sci*, 32, 2–47 (2006).
- [21] T.J. Kotas, *the Exergy Method of Thermal Plant Analysis*, Krieger Publishing Florida (1995).
- [22] J. B. Heywood, *Internal Combustion Engine Fundamentals*, New York, McGraw Hill Science, (1988).
- [23] C. R. Ferguson, *Internal combustion engine applied thermo sciences*, New York, John Wiley and Sons, (1985).
- [24] B. Najafi, R. Ebrahim zadeh, Experimental Study of The mixture Equivalence Ratio of Biodiesel, Ethanol and Gasoline in a Diesel engine, *The 5th National Conference & Exhibition on Environmental Engineering*, (2011), (In Persian).
- [25] Osmont, L. Catoire, I. Gokalp, Thermochemistry of Methyl and Ethyl Esters from Vegetable Oils, *Int. J. Chemical Kinetics*, 39, 481-491 (2007).
- [26] R. S. Benson, N. D. Whitehouse, *Internal Combustion Engines*, Pergamon Press, Oxford, (1979).
- [27] G. Woschni, Universally Applicable Equation for Instantaneous Heat Transfer Coefficient in The Internal Combustion engine, SAE Technical Paper, No. 670931. (1967).